Rationalizing oligomerization in dimethylindium(III) chalcogenolates (Me_2InER') (E = O, S, Se): A structural and computational study†

Glen G. Briand,*[a] Andreas Decken[b] and Nathan S. Hamilton[a]

Received 24th December 2009, Accepted 10th February 2010
First published as an Advance Article on the web 9th March 2010
DOI: 10.1039/b927128g

The effect on oligomerization of increased steric bulk in dimethylindium(III) chalcogenolates (Me_2InER') (E = O, S, Se) has been examined. The facile reaction of Me_3In with a series of phenols, thiophenols and selenophenols afforded the compounds $[Me_2InO(C_6H_5)]_2$ (**1**), $[Me_2InO(2,6\text{-}Me_2C_6H_3)]_2$ (**2**), $Me_2InO(2,4,6\text{-}tBu_3C_6H_3)$ (**3**), $[Me_2InS(C_6H_5)]_\infty$ (**4**), $[Me_2InS(2,4,6\text{-}tBu_3C_6H_3)]_\infty$ (**6**), $[Me_2InSe(C_6H_5)]_2$ (**7**), $[Me_2InSe(2,4,6\text{-}Me_3C_6H_3)]_\infty$ (**8**) and $[Me_2InSe(2,4,6\text{-}tBu_3C_6H_3)]_\infty$ (**9**). All compounds have been characterized by elemental analysis, melting point, FT-IR, FT-Raman, solution NMR, and X-ray crystallography. The structures of **1–2** are dimeric *via* short intermolecular In–O interactions, yielding a symmetric In_2O_2 unit and a distorted tetrahedral C_2O_2 bonding environment for indium. Increasing steric bulk in **3** results in the isolation of a monomeric species, exhibiting a distorted trigonal planar C_2O bonding environment for indium. In contrast to **1**, the thiolate analogue **4** exhibits a polymeric structure *via* μ_2-SPh groups and a distorted tetrahedral C_2S_2 bonding environment for indium. Increasing steric bulk resulted in the formation of a chain of weakly coordinated monomers *via* intermolecular In···S interactions in $[Me_2InS(2,4,6\text{-}tBu_3C_6H_2)]_\infty$ (**6**). Although **7** shows a dimeric species similar to **1**, the 2,4,6-trimethyl substituted selenolate analogue **8** exhibits a polymeric structure, while the –Se-2,4,6-$tBu_3C_6H_3$ analogue (**9**) showing a similar structure to **6**. Comparison to previously reported structures of diorganoindium chalcogenolates demonstrates the importance of the methyl substituents on indium in facilitating the isolation of higher (non-dimeric) oligomers. Theoretical calculations demonstrate the significance of altering the R and R′ groups and E on the degree of oligomerization in $[R_2InER']_n$ species.

Introduction

Semiconducting indium chalcogenide materials (*e.g.* InE and In_2E_3) have been of interest for a number of years due to their potential applications in switching devices, photovoltaics and non-linear optics.[1] Indium oxide (In_2O_3), in particular, is a transparent conducting oxide with a number of applications in thin film form, such as liquid crystal displays, gas sensors, solar cells, light emitting diodes and other optoelectronic devices.[2] In light of this, the preparation of thin films of these materials *via* metal organic chemical vapor deposition (MOCVD) involving single-source precursors has been an ongoing area of research.[3] Studies into suitable candidates for such processes have focused on a variety of indium chalcogenolate species, including diorganoindium chalcogenolates (R_2InER') (E = O, S, Se, Te).[4,5] It has been demonstrated that the size and geometry of the precursor molecular core (*i.e.* the degree of oligomerization) influences the composition, phase and morphology of the films formed by MOCVD, as do its volatility and M to E stoichiometry.

X-ray crystallographic analyses of several examples of R_2InER' compounds have shown that the vast majority of these species (as well as other group 13 analogues) are dimeric (Chart 1, n = 2) in the solid-state *via* very short intermolecular M···E bonding interactions, yielding strongly bonded and symmetric

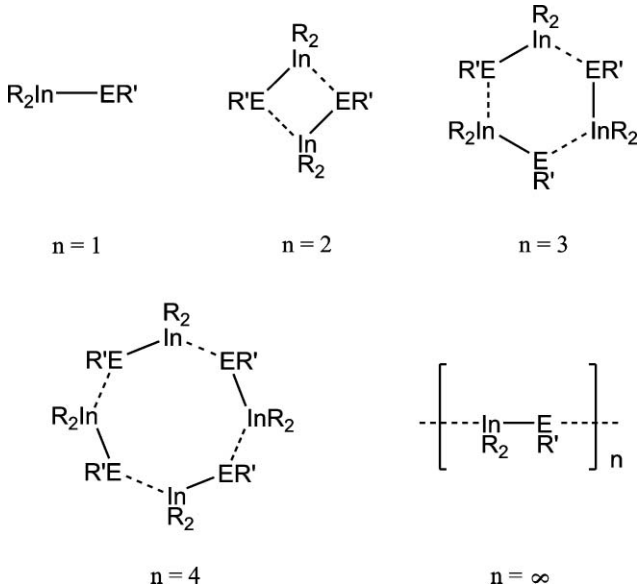

Chart 1 Schematic drawings of possible oligomers of $[R_2InER']_n$.

[a]*Department of Chemistry and Biochemistry, Mount Allison University, Sackville, New Brunswick, Canada E4L 1G8. E-mail: gbriand@mta.ca; Fax: +1 506-364-2313; Tel: +1 506-364-2346*
[b]*Department of Chemistry, University of New Brunswick, Fredericton, New Brunswick, Canada E3B 5A3*

† CCDC reference numbers 747574–747580. For crystallographic data in CIF or other electronic format see DOI: 10.1039/b927128g

In_2E_2 units.[6–10] Interestingly, a study of diorganoindium thiolate analogues (R_2InSR') produced, in addition to the expected dimeric species, the trimeric (n = 3) and tetrameric (n = 4) oligomers $[Me_2InS\text{-}tBu]_3$ and $[Me_2InS(2,6\text{-}Me_2C_6H_3)]_4$, respectively.[7a] These compounds are the only reported examples of R_2InER' compounds containing methyl substituents on indium, suggesting that minimizing steric bulk at indium may permit structural flexibility in these systems. The possibility of sterically controlling the degree of oligomerization in these species, and thus their physical and thermal decomposition properties, has been previously proposed.[11] However, there has been little in the way of systematic studies on the effect of the R/R′ substituents or the chalcogen (E) on the degree of oligomerization. Therefore, to probe the effect of altering the steric bulk and the nature of the chalcogen on the formation of intermolecular bonds and the degree of oligomerization in dimethylindium chalcogenolates, we have prepared and structurally characterized the complexes $[Me_2InO(C_6H_5)]_2$ (**1**), $[Me_2InO(2,6\text{-}Me_2C_6H_3)]_2$ (**2**), $Me_2InO(2,4,6\text{-}tBu_3C_6H_3)$ (**3**), $[Me_2InS(C_6H_5)]_\infty$ (**4**), $[Me_2InS(2,4,6\text{-}tBu_3C_6H_3)]_\infty$ (**6**), $[Me_2InSe(C_6H_5)]_2$ (**7**), $[Me_2InSe(2,4,6\text{-}Me_3C_6H_3)]_\infty$ (**8**) and $[Me_2InSe(2,4,6\text{-}tBu_3C_6H_3)]_\infty$ (**9**), which incorporate varying degrees of steric bulk in the substituted phenylchalcogenolate ligands (Chart 2). Further, we have probed the thermodynamic favorability of the various oligomers *via* theoretical calculations.

Results and discussion

Syntheses

The hydrocarbon elimination reaction between R_3In and the corresponding HER′ is desirable due to its potential general applicability to (R_2InER') (E = O, S, Se) systems, as well as the high reactivity of the trimethylindium species to rapidly yield the more stable dimethylindium chalcogenolate. Interestingly, this reaction route has not been employed previously for the preparation of R_2InSeR' analogues.[6a,6b,7] The reactions of Me_3In with HER′ in pentane, hexane, toluene or diethyl ether to yield **1–4** and **6–9** occurred rapidly at room temperature with evolution of methane gas. All reactions were stirred for 1–18 h and the products were isolated by slow evaporation or cooling of reaction mixtures. Although all reactions were quantitative, as determined from ^1H NMR spectra of the reaction mixtures, the reported yields (8–74%) are of crystalline material obtained from the reaction filtrate.

X-ray structural analyses

Crystals suitable for X-ray crystallographic analysis were isolated for **1–4** and **6–9** by the slow evaporation of reaction mixtures at 23 °C. Crystallographic data is given in Table 1. Selected bond distances and angles are given in Table 2.

Me_2In–OR′ species. Despite several attempts in various solvents, crystals of Me_2In–OPh (**1**) of sufficient quality for adequate refinement of X-ray crystallographic data could not be obtained.[12] However, preliminary data was sufficient to confirm that the compound exists as a dimer in the solid state *via* intermolecular In···O interactions, and exhibits a characteristic In_2O_2 core and a distorted tetrahedral C_2O_2 bonding environment for indium. Interestingly, the phenyl rings are coplanar with the In_2O_2 ring. The structure of $[Me_2In\text{–}O(2,6\text{-}Me_2C_6H_3)]_2$ (**2**) (Fig. 1) shows an analogous dimeric structure and a near symmetric In_2O_2 core [In1–O1 = 2.184(2) Å, In1–O1* = 2.203(2) Å]. In this case, however, the disubstituted phenyl rings are perpendicular to the In_2O_2 core, presumably to minimize steric repulsion. Alternatively, the X-ray crystallographic analysis of $[Me_2In\text{–}O(2,4,6\text{-}tBu_3C_6H_2)]$ (**3**) (Fig. 2) shows the compound to be a monomer in the solid state, with a C_2O distorted trigonal planar bonding environment at indium (Σ X–In–X = ~359°). The In–C [In1–C1 = 2.066(19) Å,

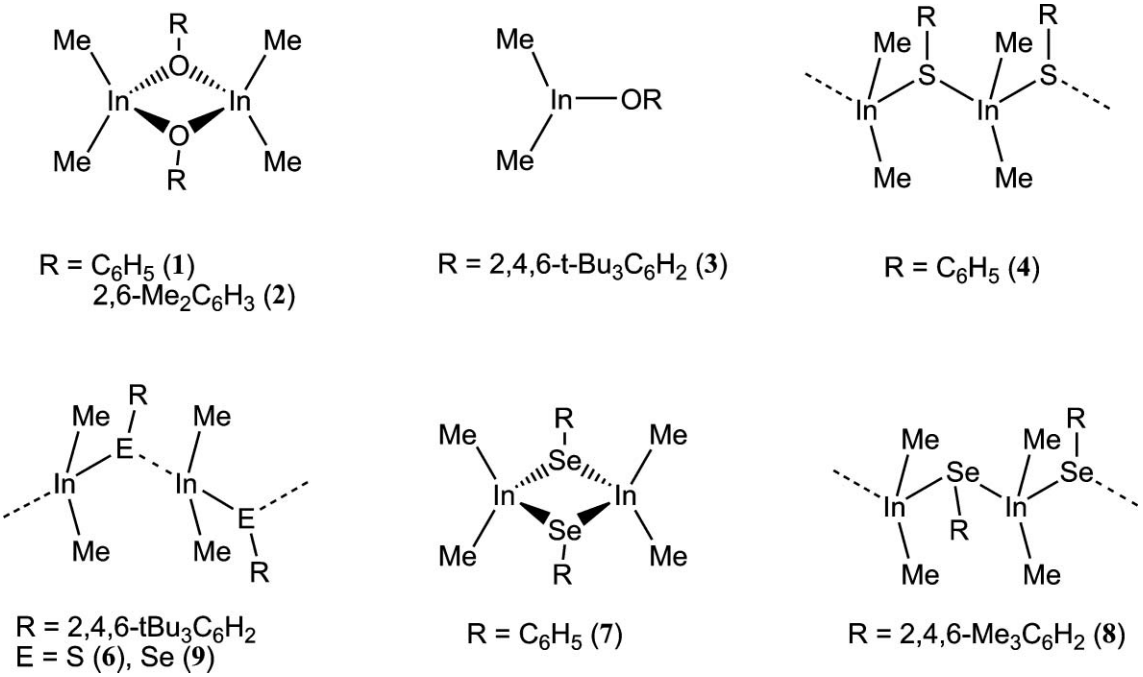

Chart 2 Schematic drawings of $[Me_2In\text{-}ER']_n$ (**1–9**).

Table 1 Crystallographic data for **2–4**, **6–9**

	2	**3**	**4**	**6**	**7**	**8**	**9**
Formula	$C_{20}H_{30}O_2In_2$	$C_{20}H_{35}OIn$	$C_8H_{11}SIn$	$C_{20}H_{35}InS$	$C_{16}H_{22}Se_2In_2$	$C_{11}H_{17}SeIn$	$C_{20}H_{35}InSe$
Fw	532.08	406.30	254.05	422.36	601.90	343.03	469.26
Crystal system	Rhombohedral	Monoclinic	Orthorhombic	Monoclinic	Monoclinic	Monoclinic	Monoclinic
Space group	$R\bar{3}$	$P2_1/m$	$Pbca$	$P2_1/c$	Pc	$Pca(2)1$	$P2_1/c$
a/Å	27.368 (6)	9.4341 (17)	12.5789 (19)	13.1942 (13)	10.9188 (15)	22.591 (3)	13.226 (3)
b/Å	27.368 (6)	9.9553 (18)	6.9213 (11)	8.9451 (9)	11.7444 (17)	7.2214 (9)	9.016 (2)
c/Å	8.447 (2)	11.237 (2)	21.401 (3)	17.4003 (17)	7.7891 (11)	7.5586 (10)	17.484 (4)
α/°	90	90	90	90	90	90	90
β/°	90	101.514 (2)	90	91.973 (1)	108.046 (2)	90	92.547 (4)
γ/°	120	90	90	90	90	90	90
V/Å^3	5479 (2)	1034.1 (3)	1863.2 (5)	2052.4 (4)	949.7 (2)	1233.1 (3)	2082.9 (9)
Z	9	2	8	4	2	4	4
$F(000)$	2376	424	992	880	568	664	952
ρ_{calcd}/g cm^{-3}	1.451	1.305	1.811	1.367	2.105	1.848	1.496
μ/mm^{-1}	1.901	1.144	2.688	1.250	6.250	4.826	2.879
T/K	198 (1)	198 (1)	198 (1)	173 (1)	173 (1)	198 (1)	173 (1)
λ/Å	0.71073	0.71073	0.71073	0.71073	0.71073	0.71073	0.71073
R_1[a]	0.0522	0.0562	0.0362	0.0220	0.0520	0.0309	0.0430
wR_2[b]	0.1549	0.2006	0.0591	0.0558	0.1264	0.0606	0.1072

[a] $R_1 = [\sum||F_o|-|F_c||]/[\sum|F_o|]$ for $[F_o^2 > 2\sigma(F_o^2)]$. [b] $wR_2 = \{[\sum w(F_o^2-F_c^2)^2]/[\sum w(F_o^4)]\}^{\frac{1}{2}}$.

Table 2 Selected bond distances (Å) and angles (°) for **2–9**

	2	**3**	**4**	**5**[7a]	**6**	**7**	**8**	**9**
In1–C1	2.137 (4)	2.066 (19)	2.148 (3)	2.159 (8)	2.140 (2)	2.178 (18)	2.145 (5)	2.134 (5)
In1–C2	2.141 (4)	2.110 (15)	2.138 (3)	2.154 (7)	2.145 (2)	2.110 (19)	2.142 (5)	2.136 (5)
In2–C3				2.135 (7)		2.157 (17)		
In2–C4				2.134 (8)		2.130 (18)		
In1–E1	2.184 (2)	2.047 (11)	2.6064 (9)		2.5755 (5)	2.786 (2)	2.7340 (7)	2.6792 (8)
In1–E1*	2.203 (2)		2.6041 (8)	2.602 (2)	2.8948 (5)		2.7328 (6)	2.9007 (8)
In1–E2				2.584 (2)		2.712 (2)		
In2–E1				2.591 (2)		2.742 (2)		
In2–E2				2.581 (2)		2.777 (2)		
C1–In1–C2	131.0 (2)	109.3 (8)	133.77 (13)	131.2 (4)	144.30 (9)	137.7 (7)	137.5 (2)	143.6 (2)
C3–In2–C4				135.0 (4)		138.2 (7)		
E1–In1–E1*	73.47 (9)		101.94 (2)		124.240 (8)		111.154 (15)	119.07 (2)
E1–In1–E2						92.61 (7)		
E1*–In1–E2				90.03 (6)				
E1–In2–E2				92.82 (6)		92.16 (7)		
In1–E1–In2						87.19 (6)		
In1–E1–In1*	106.53 (10)		108.54 (3)		139.764 (18)		120.274 (19)	144.16 (2)
In1*–E1–In2				130.47 (7)				
In1–E2–In2				123.3 (3)		88.00 (7)		

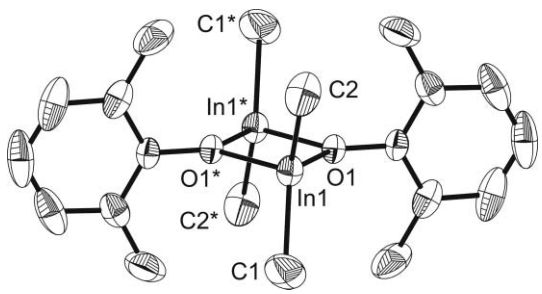

Fig. 1 X-ray structure of **2** (50% probability ellipsoids). Hydrogen atoms are not shown for clarity. Symmetry transformations used to generate equivalent atoms: (*) –x+1, –y+2, –z.

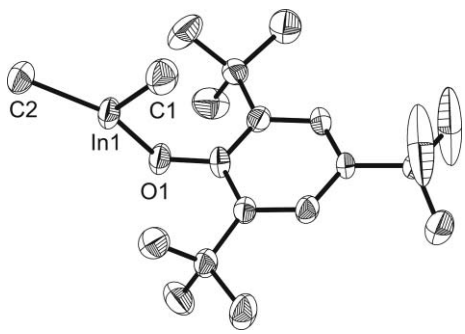

Fig. 2 X-ray structure of **3** (50% probability ellipsoids). Hydrogen atoms are not shown for clarity.

In1–C2 = 2.110(15) Å] and In–O [In1–O1 = 2.047(11) Å] bond distances are significantly shorter that those of **2** and previously reported dimeric $[R_2In–OR']_2$ analogues [In–C 2.206(18)–2.219(12) Å; In–O 2.118(2)–2.185(4) Å],[6] which is expected given the three coordinate bonding environment for indium in **3**. The nearest In···O distance is >9.5 Å and well outside of the sum of

the metallic/van der Walls radii (3.07 Å).[13] This represents the first example of a monomeric $R_2In–OR'$ complex and a rare example of a monomeric $R_2M–ER'$ (M = B, Al, Ga, In, Tl) complex.[14]

$Me_2In–SR'$ species. X-ray crystallographic analysis of $[Me_2InS(C_6H_5)]_\infty$ (**4**) (Fig. 3) shows the compound to be a polymer in the solid state *via* bridging μ_2-SPh groups, giving a four coordinate C_2S_2 bonding environment and a distorted tetrahedral geometry at indium. In–C [In1–C1 = 2.148(3) Å, In1–C2 = 2.138(3) Å] and In–S [In1–S1 = 2.6064(9) Å, In1–S1* = 2.6041(8) Å] bond distances are within the range of those of previously reported oligomeric complexes [In–C = 2.137(12)–2.23(1) Å; In–S = 2.562(4)–2.651(2) Å].[7,8] Not surprisingly, both the S1–In1–S1* [101.94(2)°] and In1–S1–In1* [108.54(3)°] bond angles of **4** are significantly larger than those observed for dimeric $[R_2In–SR']_2$ complexes. Interestingly, however, the S–In–S bond angle is significantly larger and the In–S–In bond angle is significantly smaller than those observed for the trimeric and tetrameric complexes $[Me_2In–S\text{-}tBu]_3$ and $[Me_2In–S(2,6\text{-}Me_2C_6H_3)]_4$ (**5**) [S–In–S: 90.03(6)–96.89(11)°; In–S–In 109.39(12)–130.47(7)°].[7a] As in most $R_2In–SR'$ complexes, the In–S bond distances in **4** are not significantly different and each thiolate group is equally associated with two neighbouring In atoms. A monomeric unit cannot be distinguished. Interestingly, the phenyl groups are all located on one side of the $[–In–S–]_\infty$ chain in an isotactic-type arrangement, while all dimeric R_2InSR 'show thiolate R' groups in *trans* positions in the solid state.[7,8]

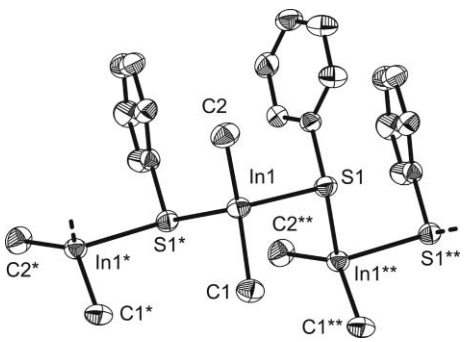

Fig. 3 X-ray structure of **4** (50% probability ellipsoids). Hydrogen atoms are not shown for clarity. Symmetry transformations used to generate equivalent atoms: (*) $-x+\frac{1}{2}, y+\frac{1}{2}, z$; (**) $-x+\frac{1}{2}, y-\frac{1}{2}, z$.

The structure of $[Me_2In–S(2,4,6\text{-}tBu_2C_6H_3)]_\infty$ (**6**) (Fig. 4) shows a polymeric structure *via* μ_2-$S(2,4,6\text{-}tBu_2C_6H_3)$ groups, similar to **4**. In this case, however, the In–S bond distances are significantly different [In1–S1 = 2.5755(5) Å, In1–S1* = 2.8948(5) Å], with In1–S1 being within the expected range and In1–S1* being ~0.2–0.3 Å longer. Further, the sum of the C1–In1–C2 [144.30(9)°], C1–In1–S1 [105.57(7)°] and C2–In1–S1 [102.53(6)°] bond angles is ~352°. This suggests a distorted trigonal planar C_2S bonding environment at In, similar to that observed in **3**, with a weak intermolecular In…S interaction [sum of metallic/van der Waals radii = 3.52 Å].[13] The polymeric structure may therefore be viewed as being composed of weakly associated monomers.

$Me_2In–SeR'$ species. The structure of $[Me_2InSe(C_6H_5)]_2$ (**7**) (Fig. 5) shows the compound to be a dimer in the solid state *via* intermolecular In···Se interactions, and exhibits a characteristic In_2Se_2 core and a distorted tetrahedral C_2Se_2 bonding environment

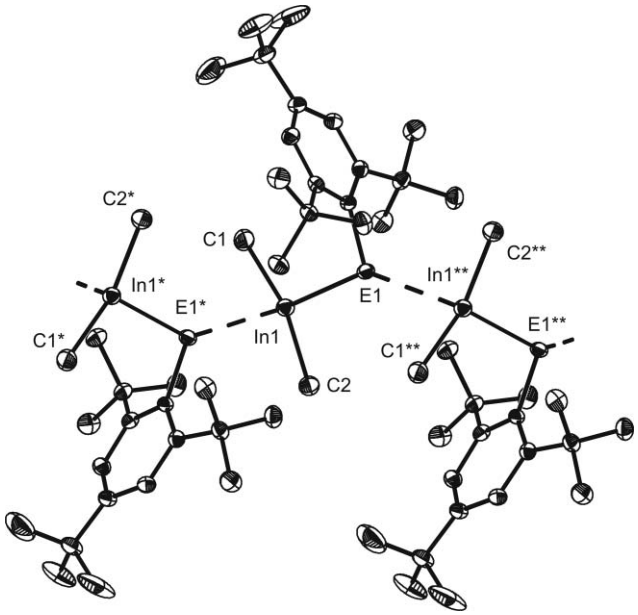

Fig. 4 X-ray structure of **6** (E = S) and **9** (E = Se) (50% probability ellipsoids). Hydrogen atoms are not shown for clarity. Symmetry transformations used to generate equivalent atoms: (*) $-x+1, y+\frac{1}{2}, -z+\frac{1}{2}$; (**) $-x+1, y-\frac{1}{2}, -z+\frac{1}{2}$.

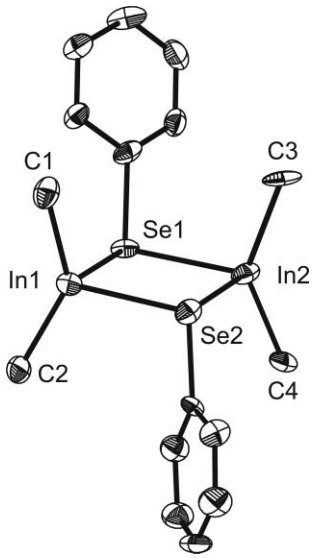

Fig. 5 X-ray structure of **7** (50% probability ellipsoids). Hydrogen atoms are not shown for clarity.

for indium. In–C bond distances [2.110(19)–2.178(18) Å] are similar to those observed in previously reported dimeric analogues [In–C = 2.16(2)–2.22(3) Å].[8b,9] However, the In–Se bond distances in the dimer [In1–Se1 = 2.786(2) and In1–Se2 = 2.712(2) Å; In2–Se1 = 2.742(2) and In2–Se2 = 2.777(2) Å] are significantly different when esd values are considered, with the longer distances being outside of the range of those previously reported [In–Se = 2.699(7)–2.756(1)].[8b,9] The differences are relatively small, however, and the compound can be considered a strongly bonded dimer.

X-ray crystallographic analysis of $[Me_2InSe(2,4,6\text{-}Me_3C_6H_2)]_\infty$ (**8**) (Fig. 6) shows the compound to be a polymer in the solid state *via* bridging μ_2-$Se(2,4,6\text{-}Me_3C_6H_2)$ groups, giving a four

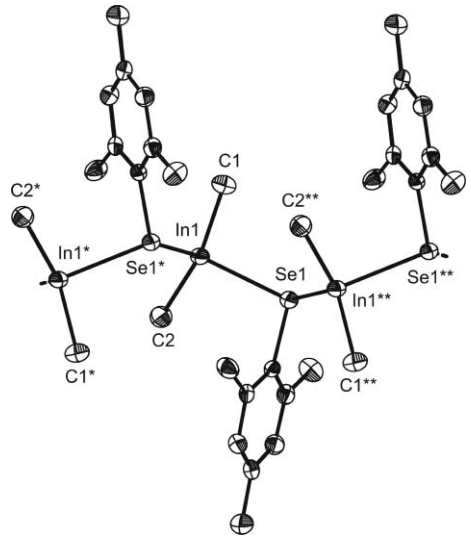

Fig. 6 X-ray structure of **8** (50% probability ellipsoids). Hydrogen atoms are not shown for clarity. Symmetry transformations used to generate equivalent atoms: (*) –x, –y, z–½; (**) –x, –y, z+½.

coordinate C_2Se_2 bonding environment and a distorted tetrahedral geometry at indium. In–C [In1–C1 = 2.145(5) Å, In1–C2 = 2.142(5) Å] and In–Se [In1–Se1 = 2.7340(7) Å, In1–Se1* = 2.7328(6) Å] bond distances are within the range of those of previously reported dimeric complexes. Not surprisingly, both the Se1–In1–Se1* [111.154(15)°] and In1–Se1–In1* [120.274(19)°] bond angles of **8** are significantly larger than those observed for dimeric $[R_2In–SeR']_2$ complexes [Se–In–Se 81.7(1)–94.06(4)°; In–Se–In 85.94(4)–98.3(1)°].[8,9] Like **4**, the In1–E1 and In1–E1* bond distances in **8** are not significantly different and each selenolate group is equally associated with two neighbouring In atoms. Unlike **4**, however, the (2,4,6-$Me_3C_6H_2$) groups alternate along the $[–In–Se–]_\infty$ chain in a syndiotactic-type arrangement.

The structure of $[Me_2InSe(2,4,6\text{-}tBu_2C_6H_3)]_\infty$ (**9**) (Fig. 4) is isostructural with that of **6**, and shows a polymeric structure *via* μ_2-Se(2,4,6-$tBu_2C_6H_3$) groups. As in **6**, the In–Se bond distances are significantly different [In1–Se1 = 2.6792(8) Å, In1–Se1* = 2.9007(8) Å], with In1–Se1 being within the expected range and In1–Se1* being ~0.2 Å longer[8b,9] [sum of metallic/van der Waals radii = 3.67 Å].[13] In this case, however, the percentage difference in In–E (8%) is not great as that of **6** (12%), suggesting a stronger secondary interaction and a more tightly bonded polymer. This is presumably a result of the larger atomic radius of Se *versus* S. Furthermore, the sum of the C1–In1–C2 [143.6(2)°], C1–In1–Se1 [105.82(18)°] and C2–In1–Se1 [102.10(16)°] bond angles is ~352°. This suggests a distorted trigonal planar C_2Se bonding environment at In, similar to that observed in **3**, with a weak intermolecular In···Se interaction. The polymeric structure may therefore be viewed as being composed of weakly associated monomers.

Computational studies

Given the varying degrees of oligomerization observed in **1–9**, and the vast majority of dimeric $[R_2InER']_2$ structures observed in the literature, a computational study was undertaken to determine the effect of varying the steric bulk of R and R′, and the identity of E, on the relative energies of $[R_2InER']_n$ (n = 1–4) systems. The geometry optimized structures resemble those of the corresponding oligomers in the solid solid-state, *i.e.* monomeric compounds show structures similar to $[Me_2InO(tBu_3C_6H_2)]$ (**3**), dimeric compounds contain planar symmetric In_2E_2 rings and ligand arrangements similar to $[Me_2InO(2,6\text{-}Me_2C_6H_3)]$ (**2**) and $[tBu_2InStBu]_2$, while trimeric and tetrameric compounds show puckered rings and ligand arrangements similar to $[Me_2InStBu]_3$ and $[Me_2InS(Me_2C_6H_3)]_4$ (**5**), respectively. Representative structures are shown in Fig. 7. The resulting electronic energy of the geometry optimized structures was divided by n to yield an energy per monomer (E/n) value, which could be directly compared to values for corresponding oligomers (*i.e.* those containing similar R, R′ and E groups). Results are presented in Table 3.

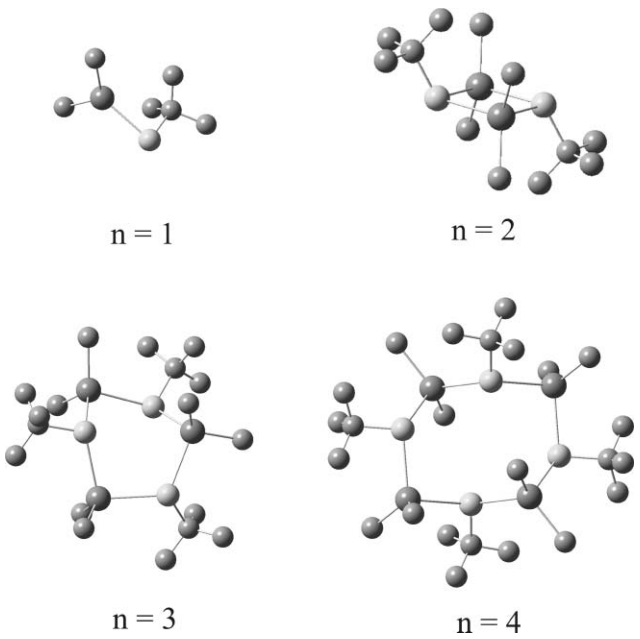

Fig. 7 Geometry optimized structures of $[Me_2InStBu]_n$ (n = 1, 2, 3 and 4).

Energies for the monomeric systems (n = 1) were found to be the largest for each compound, due to the absence of the extra intermolecular In–E bonding contacts found when n = 2–4 (see Chart 1). For $[Me_2InOMe]_n$, which contain minimal steric bulk at In and O, the E/n value is lowest for n = 2 and increases significantly for higher oligomers. This suggests a strong preference for dimeric structures when E = O, and is consistent with observed structural data. Interestingly, E/n values for the corresponding thiolate systems (*i.e.* $[Me_2InSMe]_n$) show the opposite trend, with the tetramer value being the lowest. This suggests that the $[–In–S–]_n$ ring structure is sufficiently flexible to accommodate ring strain, and that there is potential for higher (n > 2) degrees of oligomerization, as has been observed for **4–6** and other reported structures.[7a]

Given the strong preference for dimerization in E = O systems and the observed structural flexibility in the E = S analogues, the remainder of this computational study focused on thiolate oligomers. First, the effect of varying the organic group at indium (R) was studied in $[R_2InSMe]_n$ [R = Me, Ph, tBu, (2,6-$Me_2C_6H_3$); n = 1–4]. For $[Ph_2InSMe]_n$, a similar trend as for $[Me_2InSMe]_n$

Table 3 Calculated energies for geometry optimized $[R_2InER']_n$ species (E/n in parentheses) (kJ mol^{-1})

E	R	R′	n = 1	n = 2	n = 3	n = 4
O	Me	Me	148 (148)	97.0 (48.5)	207 (69.0)	294 (73.5)
S	Me	Me	223 (223)	180 (90.0)	262 (87.3)	343 (85.8)
S	Ph	Me	789 (789)	1342 (671.0)	2008 (669.3)	2675 (668.8)
S	tBu	Me	504 (504)	756 (378)	1146 (382.0)	1544 (386.0)
S	2,6-$Me_2C_6H_3$	Me	943 (943)	1744 (872.0)	2683 (894.3)	3641 (910.3)
S	Me	Ph	534 (534)	819 (410)	1221 (407.0)	1663 (415.8)
S	Me	tBu	427 (427)	599 (299)	916 (305)	1242 (310.5)
S	Me	2,6-$Me_2C_6H_3$	638 (638)	1015 (507.5)	1569 (523.0)	2092 (523.0)
S	Me	2,6-$tBu_3C_6H_2$	1046 (1046)	1938 (969.0)	2953 (984.3)	3959 (989.8)

is observed. However, introducing steric bulk at indium (R = tBu, 2,6-$Me_2C_6H_3$) results in an increase in the E/n values for higher oligomers, with the R = 2,6-$Me_2C_6H_3$ compounds showing the steepest increase. Further, [(2,6-$Me_2C_6H_3$)$_2$InSMe] shows the smallest decrease in energy on dimerization (71 kJ mol^{-1}), as compared to 118 and 126 kJ mol^{-1} for R = Ph and tBu. This suggests that an increase in steric bulk at In leads to a more highly strained system and less favorable dimeric structure. These results correspond to what has been observed in previously reported structures, where all R = tBu, Np and Mes (Np = neopentyl, Mes = 2,4,6-$Me_3C_6H_2$) systems are dimeric (no R = Ph structures have been reported).

Finally, varying steric bulk at the thiolate group (R′) was studied in $[Me_2InSR']_n$ [R′ = Me, Ph, tBu, (2,6-$Me_2C_6H_3$); n = 1–4]. As with the $[R_2InSMe]_n$ (R = tBu, 2,6-$Me_2C_6H_3$) systems, a general increase in E/n is observed with higher oligomers for all systems. Interestingly, however, the R′ = Ph systems show the lowest value for the trimer (n = 3), while the n = 3 and 4 structures show similar values when R′ = 2,6-$Me_2C_6H_3$. Again, the sharpest increases in energy with increasing n are for the bulkiest groups, with the Me_2InS(2,6-$tBu_3C_6H_2$) showing the smallest decrease in energy on dimerization (77 kJ mol^{-1}) *versus* 124–130 kJ mol^{-1} for R′ = Ph, tBu and 2,6-$Me_2C_6H_3$. Overall, these results support the observed formation of higher oligomers for $[Me_2InSR']$ systems, particular with small to intermediate sized R′ groups.

Conclusions

The effect on oligomerization of increased steric bulk in dimethylindium(III) chalcogenolates (Me_2InER') (E = O, S, Se) has been examined. The structures of **1** and **2** are dimeric *via* short intermolecular In–O interactions, while increasing steric bulk in **3** results in the isolation of a monomeric species. In contrast to **1**, compound **4** exhibits a polymeric structure *via* μ_2–SPh groups, while the S(2,4,6-$tBu_3C_6H_3$) analogue (**6**) shows a similar polymeric species to **3**, but is composed of weakly associated monomeric units. Although **7** shows a dimeric species similar to **1**, the Se(2,4,6-$Me_3C_6H_3$) analogue (**8**) exhibits a polymeric structure, while the Se(2,4,6-$tBu_3C_6H_3$) analogue (**9**) shows a similar polymeric species to **6**. This variation in oligomerization highlights the significance of the methyl substituents on indium in permitting higher (non-dimeric) oligomers in the E = S and Se structures. This is further supported by theoretical studies, which demonstrate the importance of the chalcogen (*i.e.* E = O *versus* S) and significance of altering the R and R′ groups in $[R_2InSR']_n$ species on the degree of oligomerization. To further explore intermolecular indium chalcogen bonding interactions, we are currently undertaking further structural and computational studies on oligomeric diorganoindium chalcogenolate species.

Experimental

General Considerations

Phenol (≥99.0%), 2,6-dimethylphenol (99%), 2,4,6-tri-*tert*-butylphenol (99%), thiophenol (≥99%), benzene selenol (97%), elemental sulfur (>99.5%), elemental selenium (>99%), 2,4,6-trimethylphenylmagnesium bromide (1.0 M in diethyl ether), 1-bromo-2,4,6-tri-*tert*-butylbenzene (97%), n-butyl lithium (1.6 M solution in hexanes) and anhydrous pentane (>99%), were used as received from Sigma-Aldrich. $InMe_3$ was used as received from Strem. 2,4,6-trimethylbenzeneselenol was prepared *via* a modified literature procedure, as described below.[15] 2,4,6-tri-*tert*-butylbenzenethiol and 2,4,6-tri-*tert*-butylbenzeneselenol were prepared *via* literature methods.[16] Hexane, toluene and diethyl ether were dried using an MBraun SPS column solvent purification system. Despite several attempts in various deuterated solvents, the poor solubility of compounds **6** precluded collection of useful solution $^{13}C\{^1H\}$ data.

Instrumentation

Solution ^1H, $^{13}C\{^1H\}$ and ^{77}Se NMR were recorded at 23 °C on either a JEOL GMX 270 MHz + spectrometer (270, 67.9 and 109.4 MHz, respectively), or a Varian Mercury 200 MHz + spectrometer (200 and 50 MHz; ^1H and $^{13}C\{^1H\}$, respectively), and are calibrated to the residual solvent signal. Infrared spectra were recorded as Nujol mulls on a Mattson Genesis II FT-IR spectrometer in the range 4000–400cm^{-1}. Melting points were recorded on an Electrothermal MEL-TEMP melting point apparatus and are uncorrected. Elemental analyses were performed on an elementar vario ELIII universal CHNOS analyzer, or were performed by Chemisar Laboratories Inc., Guelph, Ontario. All reactions were performed under an atmosphere of inert dinitrogen using standard Schlenk techniques.

Electron impact mass spectrometry (EI-MS) data were collected after direct insertion of the solid sample from a 1177 injection port on the Varian 3800 GC using a Varian Saturn MS/MS. An initial temperature of 35 °C was held for 3.5 min, ramped at a rate of 10 °C min^{-1} to 300 °C, and held for 5 min, for a total of 35 min. Spectra were collected in the range of m/z 50–650 at 70 eV.

Preparation of $[Me_2InO(C_6H_5)]_2$ (1). C_6H_5OH (0.176 g, 1.88 mmol) was added to a solution of $InMe_3$ (0.300 g, 1.88 mmol)

in hexane (15 mL). The solution was stirred for 1 h, followed by filtration. The filtrate was allowed to sit at 23 °C. After 1 d, the solution was filtered to yield colorless crystals of **1** (0.173 g, 0.727 mmol, 39%). Anal. Calcd for $C_{16}H_{22}O_2In_2$: C, 40.51; H, 4.64; N, 0.00. Found: C, 40.83; H, 4.73; N, <0.10. Mp 102 °C. FT-IR (cm^{-1}): 622 m, 684 w, 724 w, 756 w, 836 m, 866 w, 992 w, 1022 w, 1076 m, 1103 w, 1150 w, 1244 w, 1579 s. FT-Raman (cm^{-1}): 115 m, 140 m, 182 m, 252 w, 491 *vs*, 537 w, 580 vw, 623 vw, 753 vw, 847 w, 994 m, 1028 m, 1165 m, 1263 w, 1331 vw, 1448 vw, 1590 m, 2928 m, 2995 w, 3026 w, 3048 m, 3060 m. Solution NMR data (benzene-d_6): ^{1}H NMR, δ = 0.00 [s, 6H, Me_2InO(C_6H_5)], 6.64 [m, 2H, Me_2InO(C_6H_5)], 6.80 [m, 2H, Me_2InO(C_6H_5)], 7.08 [m, 2H, Me_2InO(C_6H_5)]. ^{13}C{^{1}H} NMR, δ = −3.5 [s, Me_2InO(C_6H_5)], 118.2 [s, Me_2InO(C_6H_5)], 119.6 [s, Me_2InO(C_6H_5)], 129.9 [s, Me_2InO(C_6H_5)], 159.9 [s, Me_2InO(C_6H_5)]. EI-MS (*m*/*z*): 94 [HOC_6H_5]$^{\bullet+}$, 145 [Me_2In]$^{\bullet+}$, 476 [dimer]$^{\bullet+}$.

Preparation of [Me_2InO(2,6-$Me_2C_6H_3$)]$_2$ (2). 2,6-$Me_2C_6H_3OH$ (0.230 g, 1.88 mmol) was added to a solution of $InMe_3$ (0.300 g, 1.88 mmol) in hexane (15 mL). The solution was stirred for 1 h, followed by filtration. The solution was allowed to sit at 23 °C for 1 d, and filtered to yield colorless crystals of **2** (0.195 g, 0.81 mmol, 43%). Anal. Calcd for $C_{20}H_{30}O_2In_2$: C, 45.28; H, 5.66; N, 0.00. Found: C, 45.33; H, 6.49; N, <0.10. Mp 180 °C. FT-IR (cm^{-1}): 582 w, 723 s, 762 m, 845 s, 893 vw, 916 vw, 970 w, 1020 w, 1093 m, 1157 w, 1203 m, 1259 m, 1589 m. FT-Raman (cm^{-1}): 119 m, 141 m, 167 m, 241 w, 314 w, 487 s, 527 m, 556 vw, 695 w, 978 vw, 1095 w, 1157 m, 1264 w, 1377 w, 1445 vw, 1591 w, 2872 w, 2923 m, 2999 w. Solution NMR data (chloroform-*d*): ^{1}H NMR, δ = −0.34 [s, 6H, Me_2InO(2,6-$Me_2C_6H_3$)], 2.27 [s, 6H, Me_2InO(2,6-$Me_2C_6H_3$)], 6.92 [d, 2H, Me_2InO(2,6-$Me_2C_6H_3$)], 6.99 [s, 1H, Me_2InO(2,6-$Me_2C_6H_3$)]. ^{13}C{^{1}H} NMR, δ = 18.9 [s, Me_2InO(2,6-$Me_2C_6H_3$)], 19.1 [s, Me_2InO(2,6-$Me_2C_6H_3$)], 121.6 [s, Me_2InO(2,6-$Me_2C_6H_3$)], 129.9 [s, Me_2InO(2,6-$Me_2C_6H_3$)], 130.0 [s, Me_2InO(2,6-$Me_2C_6H_3$)], 154.9 [s, Me_2InO(2,6-$Me_2C_6H_3$)]. EI-MS (*m*/*z*): 77 [C_6H_5]$^{\bullet+}$, 115 [In]$^{\bullet+}$, 122 [HO-2,6-$Me_2C_6H_3$]$^{\bullet+}$, 145 [Me_2In]$^{\bullet+}$, 476 [dimer]$^{\bullet+}$.

Preparation of [Me_2InO(2,4,6-$tBu_3C_6H_2$)] (3). 2,4,6-$tBu_3C_6H_2OH$ (0.492 g, 1.88 mmol) was added to a solution of $InMe_3$ (0.300 g, 1.88 mmol) in pentane (15 mL). The solution was stirred for 1 h, followed by filtration, and allowed to sit at 23 °C for 1 d. The colorless solution was then concentrated to 8 mL, and allowed to sit for 2 d at 23 °C. The solution was then filtered to yield colorless crystals of **3** (0.560 g, 1.38 mmol, 74%). Anal. Calcd for $C_{20}H_{35}OIn$: C, 59.26; H, 8.64; N, 0.00. Found: C, 58.80; H, 8.59; N, <0.10. Mp 88 °C. FT-IR (cm^{-1}): 639 vw, 690 w, 728 w, 787 w, 810 m, 880 s, 963 w, 1025 vw, 1057 w, 1115 m, 1149 w, 1192 w, 1221 m, 1266 w, 1287 w, 1581 w, 1621w. FT-Raman (cm^{-1}): 135 s, 174 *vs*, 258 w, 310 w, 487 m, 515 *vs*, 561 w, 766 vw, 807 vw, 824 w, 862 w, 931 w, 1109 vw, 1174 m, 1201 w, 1462 w, 1598 vw, 1664 m, 1840 vw, 2114 vw, 2608 vw, 2714 vw, 2852 w, 2929 *vs*, 2961 s, 3632 vw. Solution NMR data (chloroform-*d*): ^{1}H NMR, δ = −0.15 [s, 6H, Me_2InO(2,4,6-$tBu_3C_6H_2$)], 1.35 [s, 9H, Me_2InO(2,*4*,6-*t*$Bu_3C_6H_2$)], 1.41 [s, 18H, Me_2InO(*2*,4,*6*-*t*$Bu_3C_6H_2$)], 7.16 [s, 2H, Me_2InO(2,4,6-$tBu_3C_6H_2$)]. ^{13}C{^{1}H} NMR, δ = 0.4 [s, Me_2InO(2,4,6-$tBu_3C_6H_2$)], 31.9 [s, Me_2InO(2,4,6-*t*$Bu_3C_6H_2$)], 34.4 [s, Me_2InO(2,4,6-*t*$Bu_3C_6H_2$)], 35.4 [s, Me_2InO(2,4,6-*t*$Bu_3C_6H_2$)], 121.9 [s, Me_2InO(2,4,6-$tBu_3C_6H_2$)], 137.7 [s, Me_2InO(2,4,6-$tBu_3C_6H_2$)], 138.2 [s, Me_2InO(2,4,6-$tBu_3C_6H_2$)], 161.2 [s, Me_2InO(2,4,6-$tBu_3C_6H_2$)]. EI-MS (*m*/*z*): 248 [HO-2,4,6-$tBu_3C_6H_2$]$^{\bullet+}$.

Preparation of [Me_2InS(C_6H_5)]$_n$ (4). C_6H_5SH (0.207 g, 1.88 mmol) was added to a solution of $InMe_3$ (0.300 g, 1.88 mmol) in ether (15 mL). The solution was stirred for 3 h, then concentrated to 8 mL, followed by filtration. After sitting for 1 d at 23 °C, the solution was filtered to yield colorless crystals of **4** (0.217 g, 0.858 mmol, 46%). Anal. Calcd for $C_8H_{11}SIn$: C, 37.83; H, 4.33; N, 0.00. Found: C, 37.40; H, 3.92; N, <0.10. Mp 98 °C. FT-IR (cm^{-1}): 688 m, 723 s, 901 vw, 1022 w, 1080 w, 1153 w, 1261 w, 1300 vw, 1574 w. FT-Raman (cm^{-1}): 118 s, 137 s, 153 s, 170 m, 194 m, 251 vw, 278 vw, 321 vw, 422 vw, 485 *vs*, 522 m, 616 w, 695 w, 1002 s, 1024 m, 1081 m, 1118 w, 1154 m, 1181 w, 1438 w, 1577 m, 2540 vw, 2595 vw, 2924 m, 2985 m, 3018 vw, 3063 s, 3145 w. Solution NMR data (toluene-d_8): ^{1}H NMR, δ = 0.12 [s, 6H, Me_2InS(C_6H_5)], 6.89 [d, 1H, Me_2InS(C_6H_5)], 6.93 [t, 2H, Me_2InS(C_6H_5)], 7.29 [d, 2H, Me_2InS(C_6H_5)]. ^{13}C{^{1}H} NMR, δ = −3.5 [s, Me_2InS(C_6H_5)], 126.1 [s, Me_2InS(C_6H_5)], 128.9 [s, Me_2InS(C_6H_5)], 132.9 [s, Me_2InS(C_6H_5)], 133.2 [s, Me_2InS(C_6H_5)]. EI-MS (*m*/*z*): 110 [HSC_6H_5]$^{\bullet+}$, 115 [In]$^{\bullet+}$, 145 [Me_2In]$^{\bullet+}$.

Preparation of [Me_2InS(2,4,6-$tBu_3C_6H_2$)] (6). 2,4,6-$tBu_3C_6H_2SH$ (0.250 g, 0.898 mmol) was added to a solution of $InMe_3$ (0.146 g, 0.898 mmol) in toluene (8 mL). The solution was stirred for 1 h, then filtered and concentrated to 1 mL. The solution was filtered to yield colorless crystals of **6** (0.031 g, 0.0734 mmol, 8%). Anal. Calcd for $C_{20}H_{35}SIn$: C, 56.87; H, 8.35; N, 0.00. Found: C, 56.68; H, 8.59; N, <0.10. Mp 250(d) °C. FT-IR (cm^{-1}): 647 w, 693 w, 724 s, 877 m, 923 w, 1018 w, 1158 w, 1213 m, 1240 m, 1260 w, 1363 s, 1410 w, 1549 vw, 1594 m. FT-Raman (cm^{-1}): 139 s, 172 s, 255 m, 417 w, 488 s, 517 m, 565 m, 641 vw, 750 vw, 766 vw, 823 m, 926 m, 1003 w, 1028 w, 1133 m, 1158 m, 1179 m, 1201 m, 1244 w, 1285 w, 1363 vw, 1392 w, 1448 m, 1594 m, 2708 w, 2776 w, 2904 *vs*, 2922 *vs*, 2960 *vs*. Solution NMR data (thf-d_8): ^{1}H NMR, δ = −0.46 [s, 6H, Me_2InS(2,4,6-$tBu_3C_6H_2$)], 1.29 [m, 9H, Me_2InS(2,*4*,6-*t*$Bu_3C_6H_2$)], 1.60 [s, 18H, Me_2InS(*2*,4,*6*-*t*$Bu_3C_6H_2$)], 7.25 [s, 2H, Me_2InS(2,4,6-$tBu_3C_6H_2$)]. EI-MS (*m*/*z*): 277 [HS-2,4,6-$tBu_3C_6H_2$]$^{\bullet+}$.

Preparation of [Me_2InSe(C_6H_5)]$_2$ (7). A solution of C_6H_5SeH (0.295 g, 1.88 mmol) in toluene (10 mL) was added drop-wise to a solution of $InMe_3$ (0.300 g, 1.88 mmol) in toluene (15 mL). The solution was stirred for 1 h, and then concentrated to 12 mL, followed by filtration. The clear colorless solution was then layered with hexane (12 mL) and allowed to sit at 4 °C. After 2 d, the solution was filtered to yield **7** as colorless crystals (0.265 g, 0.882 mmol, 47%). Anal. Calcd for $C_{16}H_{22}Se_2In_2$: C, 31.91; H, 3.66; N, 0.00. Found: C, 31.66; H, 3.59; N, <0.10. Mp 120 °C. FT-IR (cm^{-1}): 685 m, 725 s, 772 m, 846 vw, 891 w, 961 w, 1018 w, 1065 w, 1156 m, 1572 w, 1622 w. FT-Raman (cm^{-1}): 111 s, 159 *vs*, 196 s, 207 s, 250 w, 305 w, 406 vw, 504 s, 615 w, 667 w, 1000 *vs*, 1022 m, 1067 m, 1136 m, 1155 w, 1179 w, 1436 vw, 1573 m, 2929 w, 2993 w, 3013 w, 3055 s, 3141 w. Solution NMR data (benzene-d_6): ^{1}H NMR, δ = 0.50 [s, 6H, Me_2InSe(C_6H_5)], 6.70 [d, 2H, Me_2InSe(C_6H_5)], 6.99 [d, 2H, Me_2InSe(C_6H_5)], 7.33 [d, 2H, Me_2InSe(C_6H_5)]. ^{13}C{^{1}H} NMR, δ = 32.8 [s, Me_2InSe(C_6H_5)], 128.6 [s, Me_2InSe(C_6H_5)],

130.0 [s, $Me_2InSe(C_6H_5)$], 132.3 [s, $Me_2InSe(C_6H_5)$], 138.5 [s, $Me_2InSe(C_6H_5)$]. EI-MS (*m*/*z*): 115 $[In]^{\bullet+}$, 145 $[Me_2In]^{\bullet+}$.

Preparation of [(2,4,6-$Me_3C_6H_2$)SeH]. 2,4,6-$Me_3C_6H_2MgBr$ (38.0 mL, 1 M solution in ether, 38.0 mmol) was added dropwise to a solution of elemental Se (3.99 g, 38.0 mmol) in ether (25 mL). The solution was stirred for 3 h. HCl (40 mL, 3 M) was then added dropwise, and stirred for 0.5 h. The ether layer was decanted and concentrated to 15 mL. Distillation of the orange oil under reduced pressure at 52–54 °C yield a clear, pale yellow liquid [(2,4,6-$Me_3C_6H_2$)SeH] (1.51 g, 7.99 mmol, 21%). Solution NMR data (benzene-d_6): ^{1}H NMR, δ = 2.01 [s, 1H, (2,4,6-$Me_3C_6H_2$)Se*H*], 2.12 [s, 6H, (*2*,4,*6*-$Me_3C_6H_2$)SeH], 2.15 [s, 3H, (2,*4*,6-$Me_3C_6H_2$)SeH], 6.66 [s, 2H, (2,4,6-$Me_3C_6H_2$)SeH]. $^{13}C\{^1H\}$ NMR, δ = 21.0 [s, (*2*,4,*6*-$Me_3C_6H_2$)SeH], 24.1 [s, (2,*4*,6-$Me_3C_6H_2$)SeH], 135.2 [s, (2,4,6-$Me_3C_6H_2$)SeH], 137.3 [s, (2,4,6-$Me_3C_6H_2$)SeH], 138.2 [s, (2,4,6-$Me_3C_6H_2$)SeH]. ^{77}Se NMR, δ = 26.9 [d, (2,4,6-$Me_3C_6H_2$)*Se*H, $^1J(^{77}Se\text{-}^1H)$ = 120 Hz].

Preparation of [$Me_2InSe(2,4,6\text{-}Me_3C_6H_2)]_n$ (8). A solution of 2,4,6-$Me_3C_6H_2SeH$ (0.355 g, 1.88 mmol) in hexane (5 mL) was added drop-wise to a solution of $InMe_3$ (0.300 g, 1.88 mmol) in hexane (15 mL). The mixture was stirred for 1 h, followed by filtration, and then allowed to sit at 23 °C for 1 d. The colorless solution was then concentrated to 10 mL, and allowed to sit at 23 °C. After 1 d, the solution was filtered to yield **8** as colorless crystals (0.212 g, 0.62 mmol, 33%). Anal. Calcd for $C_{11}H_{17}SeIn$: C, 38.51; H, 4.96; N, 0.00. Found: C, 38.35; H, 5.15; N, <0.10. Mp 180 °C. FT-IR (cm^{-1}): 721 s, 850 s, 1016 m, 1157 w, 1269 w, 1298 vw, 1599 w. FT-Raman (cm^{-1}): 121 s, 169 m, 333 w, 482 *vs*, 524 w, 539 w, 562 m, 591 w, 704 vw, 1019 w, 1097 vw, 1157 m, 1296 m, 1378 w, 1456 vw, 1570 vw, 1599 m, 2727 w, 2849 w, 2914 m, 2982 m. Solution NMR data (chloroform-*d*): ^{1}H NMR, δ = 0.08 [s, 6H, *Me*$_2$InSe(2,4,6-$Me_3C_6H_2$)], 2.24 [s, 3H, Me_2InSe(2,*4*,6-*Me*$_3C_6H_2$)], 2.39 [s, 6H, Me_2InSe(*2*,4,*6*-*Me*$_3C_6H_2$)], 6.88 [s, 2H, Me_2InSe(2,4,6-$Me_3C_6H_2$)]. $^{13}C\{^1H\}$ NMR, δ = 15.3 [s, *Me*$_2$InSe(2,4,6-$Me_3C_6H_2$)], 20.8 [s, Me_2InSe(2,4,6-*Me*$_3C_6H_2$)], 26.2 [s, Me_2InSe(2,4,6-*Me*$_3C_6H_2$)], 125.9 [s, Me_2InSe(2,4,6-$Me_3C_6H_2$)], 136.2 [s, Me_2InSe(2,4,6-$Me_3C_6H_2$)], 141.3 [s, Me_2InSe(2,4,6-$Me_3C_6H_2$)]. ^{77}Se NMR, δ = 31.7 [s, Me_2InSe(2,4,6-$Me_3C_6H_2$)]. EI-MS (*m*/*z*): 115 $[In]^{\bullet+}$, 145 $[Me_2In]^{\bullet+}$, 199 [Se-2,4,6-$Me_3C_6H_2]^{\bullet+}$.

Preparation of [$Me_2InSe(2,4,6\text{-}tBu_3C_6H_2)$] (9). 2,4,6-$tBu_3C_6H_2SeH$ (0.250 g, 0.768 mmol) was added to a solution of $InMe_3$ (0.123 g, 0.768 mmol) in toluene (8 mL). The solution was stirred for 1 h, then filtered and concentrated to 1 mL. The solution was filtered to yield colorless crystals of **9** (0.169 g, 0.360 mmol, 47%). Anal. Calcd for $C_{20}H_{35}SeIn$: C, 51.19; H, 7.52; N, 0.00. Found: C, 51.22; H, 7.77; N, <0.10. Mp 184 °C. FT-IR (cm^{-1}): 645 w, 718 s, 801 vw, 875 m, 898 w, 921 w, 1012 m, 1126 w, 1155 w, 1184 m, 1211 m, 1235 m, 1256 w, 1278 w, 1504 vw, 1540 w, 1587 m. FT-Raman (cm^{-1}): 140 s, 257 w, 329 vw, 475 *vs*, 524 m, 567 m, 720 w, 747 vw, 822 m, 927 m, 1013 m, 1129 m, 1157 m, 1181 w, 1201 w, 1236 vw, 1280 w, 1356 vw, 1384 vw, 1446 m, 1588 m, 2702 vw, 2768 vw, 2917 s, 2964 s, 3002 m, 3110 vw, 3179 vw. Solution NMR data (benzene-d_6): ^{1}H NMR, δ = –0.03 [s, 6H, *Me*$_2$InSe(2,4,6-$tBu_3C_6H_2$)], 1.30 [s, 9H, Me_2InSe(2,*4*,6-*tBu*$_3C_6H_2$)], 1.77 [s, 18H, Me_2InSe(*2*,4,*6*-*tBu*$_3C_6H_2$)], 7.48 [s, 2H, Me_2InSe(2,4,6-$tBu_3C_6H_2$)]. $^{13}C\{^1H\}$ NMR, δ = 0.3 [s, *Me*$_2$InSe(2,4,6-$tBu_3C_6H_2$)], 31.3 [s, Me_2InSe(2,4,6-*tBu*$_3C_6H_2$)], 32.6 [s, Me_2InSe(2,4,6-*tBu*$_3C_6H_2$)], 34.7 [s, Me_2InSe(2,4,6-*tBu*$_3C_6H_2$)], 38.7 [s, Me_2InSe(2,4,6-*tBu*$_3C_6H_2$)], 122.2 [s, Me_2InSe(2,4,6-$tBu_3C_6H_2$)], 148.2 [s, Me_2InSe(2,4,6-$tBu_3C_6H_2$)], 153.9 [s, Me_2InSe(2,4,6-$tBu_3C_6H_2$)]. EI-MS (*m*/*z*): 326 [HSe-2,4,6-$tBu_3C_6H_2]^{\bullet+}$.

X-ray Structural Analysis

Crystals of **1–4** and **6–9** were isolated from the reaction mixtures as indicated above. Single crystals were coated with Paratone-N oil, mounted using a polyimide MicroMount and frozen in the cold nitrogen stream of the goniometer. A hemisphere of data was collected on a Bruker AXS P4/SMART 1000 diffractometer using ω and θ scans with a scan width of 0.3°, and 10 s (**3**, **6**, **8**, **9**) or 30 s (**2**, **4**, **7**) exposure times. The detector distance was 5 cm. The crystals of **2** and **9** were twinned and the orientation matrixes for two components in each were determined (CELL_NOW).[17] For **3**, the molecule was disordered over two sites with equal occupancies. The data were reduced (SAINT)[18] and corrected for absorption [TWINABS[19] (**2**, **9**), SADABS[20] (**3**, **4**, **6–8**)]. The structure was solved by direct methods and refined by full-matrix least squares on F^2(SHELXTL).[21] All non-hydrogen atoms were refined using anisotropic displacement parameters. Hydrogen atoms were included in calculated positions and refined using a riding model. Lattice solvent (hexane) in **2** could not be modelled properly.

Computational methods

Semi-empirical calculations were performed using Gaussian 03 at the PM3 level. All structures were geometry optimized and structural parameters for input files were derived from crystal structure data where possible. Frequency calculations were performed on all structures and gave no imaginary frequencies. Energy values reported are the electronic energy values corrected for zero-point energies derived from frequency calculations.

Acknowledgements

We thank the following: Dan Durant for assistance in collecting solution NMR data; Dr Stephen Duffy and Martin Wightman for assistance in collecting mass spectrometry data; and the Natural Sciences and Engineering Research Council of Canada, the New Brunswick Innovation Foundation, the Canadian Foundation for Innovation and Mount Allison University for financial support.

References

1 (*a*) T. Nishino and Y. Hamakawa, *Jpn. J. Appl. Phys.*, 1977, **16**, 1291; (*b*) R. S. Becker, T. Zheng, J. Elton and M. Saeki, M., *Sol. Energy Mater.*, 1986, **13**, 97; (*c*) L. I. Man, R. M. Imanov and S. A. Semiletov, *Sov. Phys. Crystallogr.*, 1976, **21**, 255; (*d*) W.-T. Kim and C.-D. Kim, *J. Appl. Phys.*, 1986, **60**, 2631; (*e*) R. Nomura, K. Kanaya, A. Moritake and H. Matsuda, *Thin Solid Films*, 1988, **167**, L27; (*f*) A. M. Mancini, G. Micocci and A. Rizzo, *Mater. Chem. Phys.*, 1983, **9**, 29.

2 (*a*) Y. Zhang, H. Ago, J. Liu, M. Yumura, K. Uchida, S. Ohshima, S. Iijima, J. Zhu and X. Zhang, *J. Cryst. Growth*, 2004, **264**, 363; (*b*) C. Kuo, S. Lu and T. Wei, *J. Cryst. Growth*, 2005, **285**, 400; (*c*) C. Falcony, J. R. Kirtley, D. J. Dimaria, T. P. Ma and T. C. Chen, *J. Appl. Phys.*, 1985, **58**, 3556; (*d*) C. G. Granqvist, *Appl. Phys. A: Mater. Sci. Process.*, 1993, **57**, 19; (*e*) J. Lao, J. Huang, D. Wang and Z. Ren, *Adv. Mater.*, 2004, **16**, 65.

3 (*a*) M. Afzaal, D. Crouch and P. O'Brien, *Mater. Sci. Eng., B*, 2005, **116**, 391; (*b*) P. Lobinger, H. S. Park, H. Hohmeister and H. W. Roesky, *Chem. Vap. Deposition*, 2001, **7**, 105; (*c*) H. W. Kim, N. H. Kim and J. H. Myung, *J. Mater. Sci.*, 2005, **40**, 4991; (*d*) P. O'Brien, D. J. Otway and J. R. Walsh, *Chem. Vap. Deposition*, 1997, **3**, 227.

4 (*a*) A. N. MacInnes, M. B. Power and A. R. Barron, *Chem. Mater.*, 1992, **4**, 11; (*b*) A. N. MacInnes, M. B. Power and A. R. Barron, *Chem. Mater.*, 1993, **5**, 1344; (*c*) S. L. Stoll, G. Gillan and A. R. Barron, *Chem. Vap. Deposition*, 1996, **2**, 182; (*d*) E. G. Gillan and A. R. Barron, *Mater. Res. Soc. Symp. Proc.*, 1996, **415**, 87; (*e*) A. N. MacInnes, M. B. Power, A. F. Hepp and A. R. Barron, *J. Organomet. Chem.*, 1993, **449**, 95.

5 (*a*) A. R. Barron, *Adv. Mater. Opt. Electron.*, 1995, **5**, 245 and references therein; (*b*) P. O. O'Brien and S. Haggata, *Adv. Mater. Opt. Electron.*, 1995, **5**, 117 and references therein; (*c*) H. J. Gysling and A. A. Warnberg, *Chem. Mater.*, 1992, **4**, 900; (*d*) J. Y. Cho, H.-C. Jeong, K.-S. Kim, D. H. Kang, H.-K. Kim and I.-W. Shim, *Bull. Korean Chem. Soc.*, 2003, **24**, 645.

6 (*a*) O. T. Beachley, D. J. MacRae and A. Y. Kovalevsky, *Organometallics*, 2003, **22**, 1690; (*b*) M. Häußlein, H. D. Hausen and J. W. Klinkhammer, *Z. Anorg. Allg. Chem.*, 1999, **625**, 1608; (*c*) T. J. Trentler, S. C. Goel, K. M. Hickman, A. M. Viano, M. Y. Chiang, A. M. Beatty, P. C. Gibbons and W. E. Buhro, *J. Am. Chem. Soc.*, 1997, **119**, 2172; (*d*) D. C. Bradley, D. M. Frigo, M. B. Hursthouse and B. Hussain, *Organometallics*, 1988, **7**, 1112.

7 (*a*) B. Yearwood, S. U. Ghazi, M. J. Heeg, N. Richardson and J. P. Oliver, *Organometallics*, 2000, **19**, 865; (*b*) H. Rahbarnoohi, M. Taghiof, M. J. Heeg, D. G. Dick and J. P. Oliver, *Inorg. Chem.*, 1994, **33**, 6307.

8 (*a*) H. Rahbarhooni, R. L. Wells, L. M. Liable-Sands, G. P. A. Yap and A. L. Rheingold, *Organometallics*, 1997, **16**, 3959; (*b*) S. L. Stoll, S. G. Bott and A. R. Barron, *J. Chem. Soc., Dalton Trans.*, 1997, 1315.

9 (*a*) H. Rahbarnoohi, R. Kumar, M. J. Heeg and J. P. Oliver, *Organometallics*, 1995, **14**, 3869; (*b*) O. T. Beachley, J. C. Lee, H. J. Gysling, S.-H. L. Chao, M. R. Churchill and C. H. Lake, *Organometallics*, 1992, **11**, 3144.

10 H. Rahbarnoohi, R. Kumar, M. J. Heeg and J. P. Oliver, *Organometallics*, 1995, **14**, 502.

11 J. P. Oliver, *J. Organomet. Chem.*, 1995, **500**, 269 and references therein.

12 Crystal data for **1**: $C_{16}H_{22}In_2O_2$, fw 475.98, monoclinic, space group *C* 1 2/m 1 (no. 12), $a = 13.9545(17)$ Å, $b = 9.8570(17)$ Å, $c = 14.232(3)$, $\alpha = 90°$, $\beta = 114.23(0)°$, $\gamma = 90°$, $V = 1785.15(50)$ Å^3, $Z = 4$, $\rho_c = 1.771$ g cm^{-3}.

13 (*a*) A. Bondi, *J. Phys. Chem.*, 1964, **68**, 441; (*b*) I. D. Brown, *Chem. Soc. Rev.*, 1978, **7**, 359.

14 (*a*) G. J. P. Britovsek, J. Ugolotti and A. J. P. White, *Organometallics*, 2005, **24**, 1685; (*b*) M. E. Gurskii, K. A. Lyssenko, A. L. Karionova, P. A. Belyakov, T. V. Potapova, M. Yu, Y. Antipin and Yu. N. Bubnov, *Izv. Akad. Nauk SSSR, Ser. Khim.(Russ.) (Russ. Chem. Bull.)*, 2004, 1884; (*c*) M. T. Ashby and N. A. Sheshtawy, *Organometallics*, 1994, **13**, 236; (*d*) R. Wehmschulte, K. Ruhlandt-Senge, M. M. Olmstead, M. A. Petrie and P. P. Power, *J. Chem. Soc., Dalton Trans.*, 1994, 2113; (*e*) W. M. Cleaver and A. R. Barron, *Organometallics*, 1993, **12**, 1001; (*f*) W. Uhl, T. Spies and R. Koch, *J. Chem. Soc., Dalton Trans.*, 1999, 2385; (*g*) R. J. Wehmschulte, K. Ruhlandt-Senge and P. P. Power, *Inorg. Chem.*, 1995, **34**, 2593.

15 M. Bochmann, K. J. Webb, M. B. Hursthouse and M. Mazid, *J. Chem. Soc., Dalton Trans.*, 1991, 2317.

16 M. Bochmann, K. J. Webb, M. A. Mailk, J. R. Walsh and P. O'Brien, *Inorg. Synth.*, 1997, **31**, 158.

17 *CELL_NOW*, 2005 George Sheldrick, Bruker AXS, Inc., Madison, Wisconsin, USA.

18 *SAINT 7.23A*, 2006, Bruker AXS, Inc., Madison, Wisconsin, USA.

19 *TWINABS 1.05*, George Sheldrick, 2004, Bruker Nonius, Inc., Madison,Wisconsin, USA.

20 *SADABS* 2004, George Sheldrick, 2004, Bruker AXS, Inc., Madison,Wisconsin, USA .

21 *SHELX 6.14*, George Sheldrick, 2000, Bruker AXS, Inc., Madison,Wisconsin, USA.